

# Green Electrospun Silk Fibroin Nanofibers Loaded with Cationic Ethosomes for Transdermal Drug Delivery

HONG Huoyan<sup>#</sup>, ZHANG Dongdong<sup>#</sup>, LIN Si, HAN Feng, WANG Kaili, JIANG Di, WU Jinglei<sup>✉</sup>, MO Xiumei and WANG Hongsheng<sup>✉</sup>

Received March 3, 2021  
 Accepted April 12, 2021  
 © Jilin University, The Editorial Department of Chemical Research in Chinese Universities and Springer-Verlag GmbH

**T**ransdermal drug delivery system (TDDS) facilitates the controlled release of active ingredients penetrating through the skin, avoiding the liver first pass effect. Electrospinning is a simple process to fabricate ultrafine fibers with a higher specific surface area, making them excellent candidates for drug delivery. In current work, a novel silk fibroin (SF) nanofiber loaded with cationic ethosomes (CEs) was prepared *via* green electrospinning. The data of Fourier transform infrared spectroscopy (FTIR) and laser scanning confocal microscopy (LSCM) confirmed the existence of CE in the SF nanofibers. The morphology of the nanofibers was not significantly affected by the incorporation of CE as shown by scanning electron microscopy (SEM) images. The CE-loaded SF nanofibrous patch (CEs-SFnP) showed good cytocompatibility as proved by both cell counting kit-8 (CCK-8) assay and SEM. Using doxorubicin hydrochloride (Dox) as a model drug, the transdermal performance of CE-SFnP was evaluated through Franz diffusion cell against mouse skin. The results indicated that CE-SFnP can effectively deliver drug into the skin, with a much higher permeation rate than the normal nanofibers without CE. The as-spun CE-SFnP in this study could find promising applications in TDDS.

**Keywords** Transdermal drug delivery; Silk fibroin; Ethosome; Green electrospinning

## 1 Introduction

Transdermal drug delivery system (TDDS) offers an advantageous alternative to conventional means of drug administration by avoiding the hepatic first pass-metabolism and the adverse reaction of gastrointestinal tract, reducing the frequency of dose and prolonging the effective time<sup>[1]</sup>. However, limited by the barrier properties of the stratum corneum and physicochemical property of the drug itself, most drugs, especially for those whose molecular weight is more than 500, cannot meet the requirements of clinical treatment through percutaneous delivery<sup>[2]</sup>. To improve the skin permeation rate is the key for the development of TDDS. In

recent years, facilitated by the application of nanotechnology, drug-loaded liposomes, ethosomes (Eth), and non-ionic surfactant, could be imported into the skin conveniently<sup>[3,4]</sup>. Eths, a modified form of liposomes that contain a relatively high concentration of ethanol, have been reported more efficient in delivering agents into the skin, in terms of quantity and depth, than liposomes or hydroalcoholic solutions<sup>[3,4]</sup>. The cationic Eths (CEs) have better performance on penetrating into the skin cells, as the surface of the cell membrane is negatively charged<sup>[5]</sup>. It was reported that drug-loaded liposome fixed on scaffolds showed steady and durable release kinetic<sup>[5]</sup>. Since CE is a special liposome, and has better transdermal performance, we hypothesized that CE-loaded scaffolds may have a good potential serving in TDDS.

Electrospun nanofibers have a unique property of large specific surface area, making it a good drug carrier<sup>[6]</sup>. Drug-loaded electrospun nanofibers have been utilized to carry various drugs, such as paclitaxel<sup>[7]</sup>, nerve growth factor<sup>[8]</sup>, and vitamins<sup>[9]</sup>. Even dual active molecules could be released simultaneously from nanofibers with well-maintained bioactivity<sup>[10]</sup>. Reasonably, the CE-loaded nanofibers can make a good TDDS, as its high specific surface area could provide more contact opportunities for CE and skin cells to obtain a higher transdermal efficiency as well as a steady and durable drug release behavior.

In addition to the skin permeation rate, the skin affinity is another key factor that needs to be considered when constructing a TDDS. Silk fibroin (SF), a main component of silkworm cocoons, has good biocompatibility, which makes it an excellent biomaterial widely used in biomedical area<sup>[11,12]</sup>. In our previous work<sup>[9,13–15]</sup>, we successfully produced drug-loaded SF nanofibrous matrices through a green process of aqueous electrospinning. Moreover, SF is favored by skin with diverse properties, such as maintaining aqueous environment for skin and good oxygen and water vapor permeability<sup>[11,12]</sup>. Therefore, SF nanofibers can be an excellent substrate for TDDS.

Herein, we aimed to fabricate a novel TDDS based on the CE-loaded SF (CEs-SF) nanofibrous patch (CEs-SFnP) *via* a green electrospinning. The CE was prepared *via* a thin-film hydration method and characterized on a laser particle analyzer, a zeta potentials instrument and a transmission

✉ WANG Hongsheng  
whs@dhu.edu.cn

✉ WU Jinglei  
jw@dhu.edu.cn

<sup>#</sup> These authors contributed equally to this work.

Key Laboratory of Science & Technology of Eco-Textile, Ministry of Education, Shanghai Engineering Research Center of Nano-Biomaterials and Regenerative Medicine, College of Chemistry, Chemical Engineering and Biotechnology, Donghua University, Shanghai 201620, P. R. China

electron microscope(TEM). The CEs-SFnP was characterized by means of Fourier transform infrared spectroscopy(FTIR), X-ray diffraction(XRD), thermal gravimetric analysis(TGA), scanning electron microscopy(SEM) and laser scanning confocal microscopy(LSCM). With doxorubicin hydrochloride(Dox) as a model drug encapsulated in CEs, the transdermal performance of the CEs-SFnP(Dox@CEs-SFnP) was evaluated with the classic method of Franz diffusion cell. The skin compatibility of CEs-SFnP was also assessed *in vitro* by fluorescence microscopy, SEM and cell counting Kit-8(CCK-8) methods.

## 2 Experimental

### 2.1 Materials

Cocoons of *Bombyx mori* silkworm were kindly supplied by Jiaying Silk Co.(China). Phosphatidylcholine, cholesterol, 3,3'-dioctadecyloxycarbocyanine(DiO) and polyethylene oxide (PEO) were purchased from Sigma-Aldrich(USA). CCK-8 and Calcein-AM/PI Double Stain Kit were purchased from Biyuntian Biotechnology Co., Ltd.(Shanghai, China). Mouse fibroblasts(L929) were obtained from Institute of Biochemistry and Cell Biology(Chinese Academy of Sciences, China). Dulbecco's modified Eagle medium(DMEM), penicillin/streptomycin and fetal bovine serum(FBS) were purchased from Gibco Life Technologies Co.(USA).

### 2.2 Preparation and Characterization of CEs

#### 2.2.1 Preparation

CEs were prepared according to the thin-film hydration method as described previously<sup>[16,17]</sup>. Briefly, 140 mg of phosphatidylcholine, 14 mg of cholesterol and 5.6 mg of octadecylamine were dissolved in 10 mL of ethanol in a flask. The solvent was removed to obtain a lipid film by rotary evaporation at 50 °C. Then, 10 mL of ethanol aqueous solution (ethanol:water=7:3 in volume ratio) containing 0.1 mg of DiO or 0.5 mg of Dox(as a model drug) was added to the flask, followed by 1 h of shaking at room temperature. After centrifugation(at 12000 r/min and 4 °C for 60 min) to remove the free DiO or Dox, homogeneous DiO-labeled CEs(DiO@CEs) and Dox-loaded CEs(Dox@CEs) were obtained using a probe sonicator(JY92-II, NingBo Scientz Biotechnology Co., Ltd., Ningbo, China) under the following conditions: power 40 W, working time 10 s, interval time 3 s, 45 cycles. The solution was then filtered with a 220 nm microporous filter membrane several times to obtain CEs with a uniform particle size.

#### 2.2.2 Characterization

The polydispersity index(PDI), electric potential and diameter

of the CEs were determined on a Zetasizer Nano ZS(ZEN3600, Malvern Panalytical Ltd., U.K.). The CEs were also observed with SEM(Phenom XL, Netherlands) and TEM(JEM-2100, JEOL Ltd., Japan).

The encapsulation efficiency(EE) of CEs was determined by ultracentrifugation using Dox as a model drug. Briefly, drugs-loaded CEs solution was centrifuged at 12000 r/min for 1 h at 4 °C. Then, the absorbance value of the supernatant at 480 nm was detected on a UV-Vis spectrophotometer (UV1100, TECHCOMP, China) and the dose of free drugs was calculated according to the standard curve(Fig.S1, see the Electronic Supplementary Material of this paper) obtained by accurately preparing a series of drug standard solutions with concentration gradients and detecting the corresponding absorbance values. Finally, EE of CEs was obtained by the following formula:

$$EE(\%)=(D_t-D_f)/D_t \times 100\% \quad (1)$$

where  $D_t$  is the total dosage added during preparation of drug-loaded CEs;  $D_f$  is the amount of free drug not encapsulated in CEs.

### 2.3 Preparation and Characterization of CEs-SFnP

#### 2.3.1 Preparation

The preparation of regenerated SF was described previously. Briefly, raw silk was degummed three times with sodium carbonate(0.02 mol/L  $\text{Na}_2\text{CO}_3$ ) solution at 100 °C for 30 min each. Subsequently, the degummed silk was dried in a drying oven to remove the water. Dry silk was dissolved in the ternary system of  $\text{CaCl}_2/\text{H}_2\text{O}/\text{EtOH}$ (1:8:2 in molar ratio) solution for 1 h at 70 °C. After dialyzed against distilled water using a cellulose tube(250-7u, Sigma, USA) at room temperature for 3 d, the SF solution was filtered to remove impurities and then put into a freeze dryer(GT2-B, SRK, Germany). SF sponges were obtained after lyophilization at -58 °C for 72 h.

The CEs were encapsulated into SF nanofibers *via* green electrospinning to obtain CEs-SFnP. Different volumes of the prepared CEs solution were added to the SF aqueous solution to generate a homogeneous blending solution with gentle stirring(the final volume ratios of CEs solution to SF solution were 0, 10%, 20%, 40% and 50%, respectively). A small amount of PEO was added to improve the spinnability of the SF aqueous solution(Table 1). The prepared solution was then

**Table 1 Formulations of blending solution for different products**

Sample	$m(\text{SF})/\text{g}$	$m(\text{PEO})/\text{g}$	$V(\text{CEs})/\text{mL}$	$V(\text{H}_2\text{O})/\text{mL}$
SFnP	1	0.1	0	5.0
CEs(10%)-SFnP	1	0.1	0.5	4.5
CEs(20%)-SFnP	1	0.1	1.0	4.0
CEs(40%)-SFnP	1	0.1	2.0	3.0
CEs(50%)-SFnP	1	0.1	2.5	2.5

electrospun at a stable extruding rate of 0.3 mL/h under a voltage of 20 kV, and the collect distance was 20 cm. The electrospun Dox@CEs-SFnPs and Dox-loaded SFnPs without CE(S) (Dox@SFnPs) were also prepared for the subsequent comparative study of transdermal performance.

### 2.3.2 Characterization

The morphology of the CE-SFnP was observed with on an SEM(Phenom XL, Netherlands) at an accelerated voltage of 10 kV. The samples were dried and sputtered coated with gold. The mean fiber diameters were determined by image analysis software(ImageJ, National Institutes of Health) and calculated by selecting 100 fibers randomly on SEM images. The distribution of CE(s) (labeled by DiO, which could emit green light while excited at 484 nm) in the nanofibers was determined on a laser scanning confocal microscope(LSCM, Zeiss LSM 700, Germany).

An FTIR(Nicolet-760, Thermo fisher, USA) spectrometer was used to collect the spectra of the samples in the range of 400–4000  $\text{cm}^{-1}$ . An XRD instrument(D8 Discover, Bruker AXS, Germany) was used to examine the crystallinity of samples at a  $2\theta$  degree between  $10^\circ$  and  $60^\circ$ . The thermal stability of the samples was investigated on a TGA instrument(TG209F1 Libra, Germany) in the range 25–600  $^\circ\text{C}$  with a heating rate of 10  $^\circ\text{C}/\text{min}$ .

### 2.4 Biocompatibility of CE-SFnP

Mouse fibroblasts(L929) were cultured in DMEM with 10% FBS and 1%(volume ratio) penicillin/streptomycin in an atmosphere of 5%  $\text{CO}_2$  at 37  $^\circ\text{C}$ . The medium was refreshed every other day. The CE-SFnPs were cut into circular pieces(14 mm in diameter), which were then placed into the wells of a 24-well plate individually and fixed with stainless steel rings. Before cells seeding, the patches were sterilized by 75%(volume ratio) ethanol vapor for 24 h as previously described<sup>[9,13–15]</sup>. Then cells were seeded onto the patches at a density of  $2 \times 10^4$  cells/well. Coverslips seeded cells were used as control.

Cell viabilities grown on different substrates were determined by CCK-8 assay. After 1, 3, 5, and 7 d of culture, the medium was replaced with 400  $\mu\text{L}$  of fresh RPMI 1640 medium(without FBS and penicillin/streptomycin) containing 40  $\mu\text{L}$  of CCK-8 solution at 37  $^\circ\text{C}$  in the dark for 1 h. Then, 100  $\mu\text{L}$  of the solution was drawn and placed into a 96-well plate. Finally, a microplate reader(Multiskan MK3, Thermo, USA) was used to detect the absorbance at 450 nm. The following formula was used to calculate the cell survival rate:

$$\text{Cell viability(\%)} = (A_t - A_b) / (A_c - A_b) \times 100\% \quad (2)$$

where,  $A_t$ : absorbance of the tested samples;  $A_b$ : absorbance of

the blank wells containing culture medium and CCK-8 solution but without cells;  $A_c$ : absorbance of controls.

Cell morphology was examined by SEM after 3 d of culture. The samples were rinsed twice with PBS and fixed with 4% glutaraldehyde aqueous solution at 4  $^\circ\text{C}$  for 2 h. The fixed samples were rinsed twice with PBS and then dehydrated in gradient concentrations of ethanol(30%, 50%, 70%, 80%, 90%, 95% and 100%). After being dried *in vacuum* oven overnight, the cellular constructs were coated with a gold sputter and observed under the SEM at a voltage of 10 kV. Fluorescence microscopy was also conducted as complements to observe cell morphology. Briefly, the paraformaldehyde-fixed cells were treated with 0.1% Triton solution for 3–5 min and washed 3 times with PBS. Then, the samples were treated with 2 mg/L bovine serum albumin(BSA) solution for 20–30 min and washed with PBS 3 times. Phalloidin was added to stain the cells for 30 min in the dark and washed with PBS 3 times. Subsequently, DAPI was added to the stain for 5 min in the dark. After washing with PBS for 3 times, the morphology of cells was observed under a fluorescence microscope(IX71, Olympus, Japan).

### 2.5 Transdermal Assays

The classic Franz diffusion cell assay was used to *in vitro* assess the transdermal performance of the CE-SFnPs. The abdomen skin of an adult mouse(4 weeks old) was shaved and peeled off after the mouse was executed(performed according to the guidelines approved by the Institutional Animal Care and Use Committee at Donghua University, China) and rinsed with sterile PBS(pH=7.4). The unbroken skin was then stored at –20  $^\circ\text{C}$  for further use. The prepared skin was sandwiched between the donor and the receiving pool of the Franz diffusion cells, and the CE-SFnPs loaded with Dox(Dox@CE-SFnPs) were tightly attached to the surface of the skin(the surface of stratum corneum facing up). The receiving pool was filled with PBS(pH=7.4), which was stirred continuously at 350 r/min and maintained at the temperature of 33  $^\circ\text{C}$  by water bath. At appropriate intervals (0.5, 1, 2, 4, 6, 8, 10, 12, 24, 36, and 48 h, respectively), 2 mL of the receiving solution was withdrawn *via* the sampling port and then replaced by equal volume of fresh PBS. The absorbance value of the receiving solution was determined with a UV-Vis spectrophotometer(UV1100, TECHCOMP, China) at 480 nm, and the cumulative drug permeation( $Q$ , %) through the skin was calculated according to the standard curve and the following formula:

$$Q(\%) = \frac{Vc_n + \sum_{i=1}^{n-1} c_i V_i}{Q'} \times 100\% \quad (3)$$

where  $V$  is the volume of the transdermal cup,  $c_n$  is the drug concentration of the receiver solution at each test time,  $c_i$  is the drug concentration of the  $i$ th sample and  $Q'$  is the total amount

of drug in the CEs-SFnPs.

The skin was removed from the Franz diffusion cells and made into paraffin sections after the above process. The distribution of Dox in the skin section was observed with an LSCM(Carl Zeiss, LSM 700, Germany).

## 2.6 Statistical Analysis

All the data were obtained at least in triplicate and all values were reported as the mean and standard deviation(SD). Statistical analysis was carried out by the one-way analysis of variance(one-way ANOVA) using Origin 8.0(OriginLab Inc., USA). A *P* value of < 0.05 is considered significant, and the data are represented by \* for *P*<0.05, \*\* for *P*<0.01.

## 3 Results and Discussion

### 3.1 Characterization of CEs

The TEM image showed that the CEs have a polygon shape and a multiwall structure with a diameter of about 78 nm (Fig.1). The PDI of the CEs was 0.164, indicating an uniform dispersion, which was also confirmed by the SEM image (Fig.S2, see the Electronic Supplementary Material of this paper). The CEs were positively charged with an average charge of about +20 mV. The particle size and electric potential of the CEs did not change significantly after being placed at 4 °C for 4 weeks[Fig.1(D) and(E)], indicating that CEs have

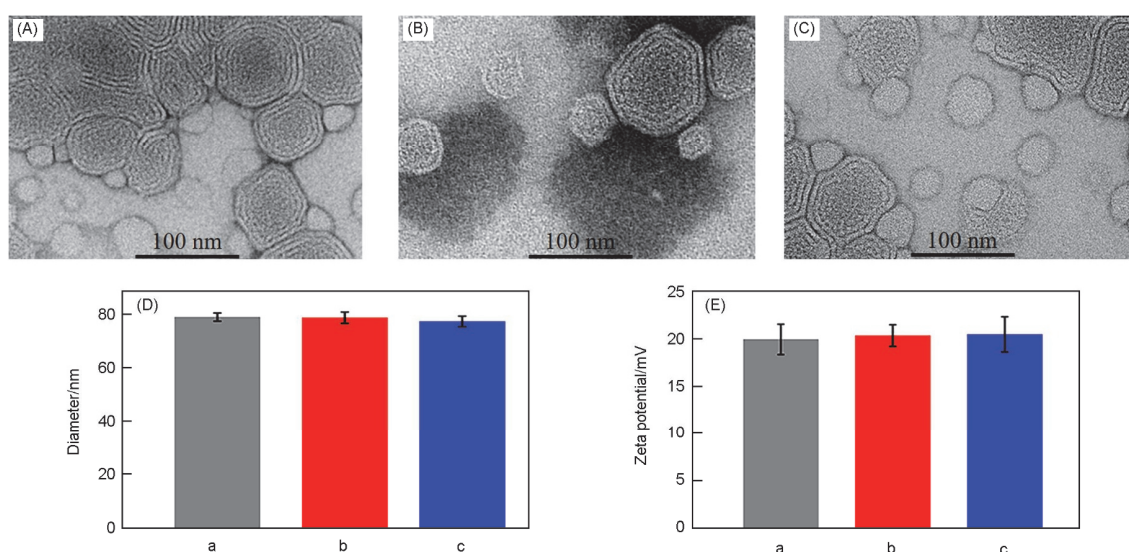


**Fig.1 TEM images(A—C), diameters(D) and potentials(E) of CEs** (A) and a. new; (B) and b. 1 week at 4 °C; (C) and c. 4 weeks at 4 °C.

good stability. With a small size and positive charge on the surface, it is conducive for CEs to adhere to the cell membrane and integrate into cells. Using Dox as the model drug, the encapsulation efficiency of the CEs was  $86.11\% \pm 0.78\%$  (Table S1, see the Electronic Supplementary Material of this paper).

### 3.2 Characterization of CEs-SFnP

The morphology of the electrospun CEs-SFnP was observed by SEM. As shown in Fig.2, the CEs-SF nanofibers have a round shape with a smooth surface. The diameter of the composite nanofibers is about 500 nm and slightly increased with the increase of CEs. However, when the volume ratio of CEs in the mixed spinning solution is up to 50%, electrospinning cannot be carried out. These results indicate that in a certain range (volume ratio < 50%), the introduction of CEs has no significant effect on morphology of the SF nanofibers. As more drug loading is advantageous for practical use, CEs ratio of 40% was

selected in the subsequent transdermal experiment.

Fig.3(A) shows the FTIR spectra of CEs-SFnP. The CEs have characteristic peaks at 2927, 2857, 1743, 1467, 1158 and 1080  $\text{cm}^{-1}$ , referring to C—H stretch,  $\text{CH}_2$  symmetrical stretch, C=O stretch,  $\text{CH}_2$  shear vibration, CO—C—O anti-symmetric expansion and  $\text{PO}_2$  symmetrical stretch of phosphatidylcholine, respectively<sup>[18]</sup>. The characteristic absorption peaks of SF are at 1650—1660  $\text{cm}^{-1}$  (amide I), 1535—1545  $\text{cm}^{-1}$  (amide II), 1235—1240  $\text{cm}^{-1}$  (amide III) and 969  $\text{cm}^{-1}$  (amide IV), representing random curl. The characteristic absorption peaks, with the characteristic absorption peaks at 1625—1640, 1515—1525, 1265, and 696  $\text{cm}^{-1}$  representing  $\beta$ -sheets<sup>[19]</sup>. The spectrum of CEs-SF exhibited typical characteristic peaks of CEs (at 1739, 1467, 1237, and 1066  $\text{cm}^{-1}$ ), which indicate that the CEs had been successfully encapsulated into the SF nanofibers. The distribution of CEs in the SF nanofibers was also confirmed by means of fluorescent microscopy. As shown in Fig.3(B), the DiO-labeled CEs were evenly distributed in the SF nanofibers.

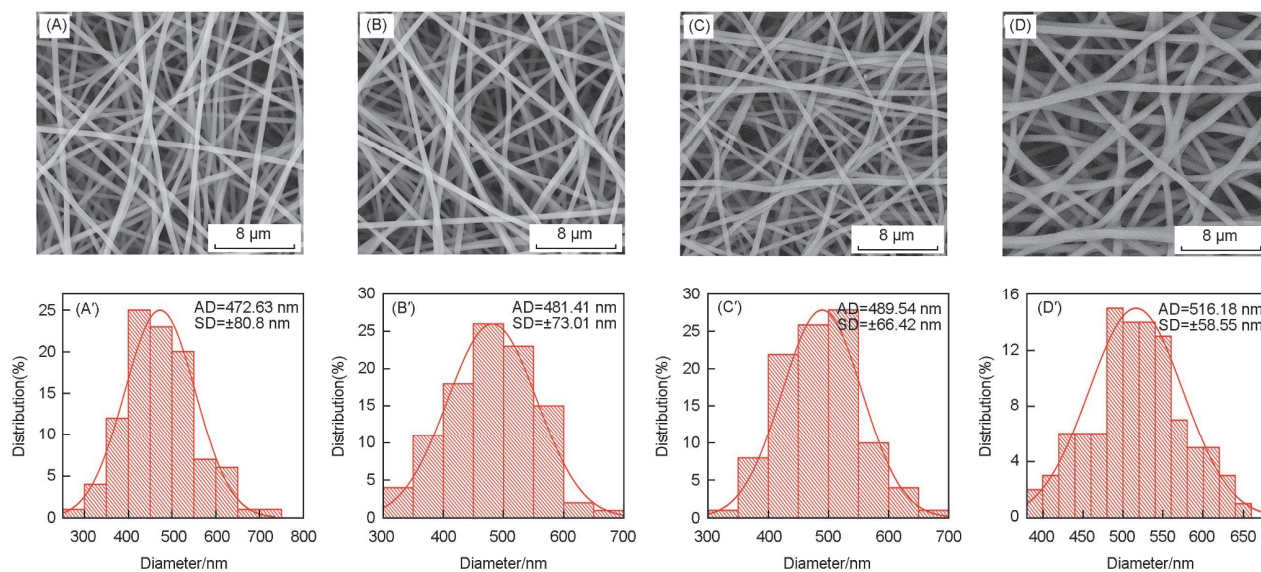


**Fig.2** SEM images(A—D) and diameter distribution(A'—D') of SF(A, A'), CE(10%)-SF(B, B'), CE(20%)-SF(C, C') and CE(40%)-SF(D, D')

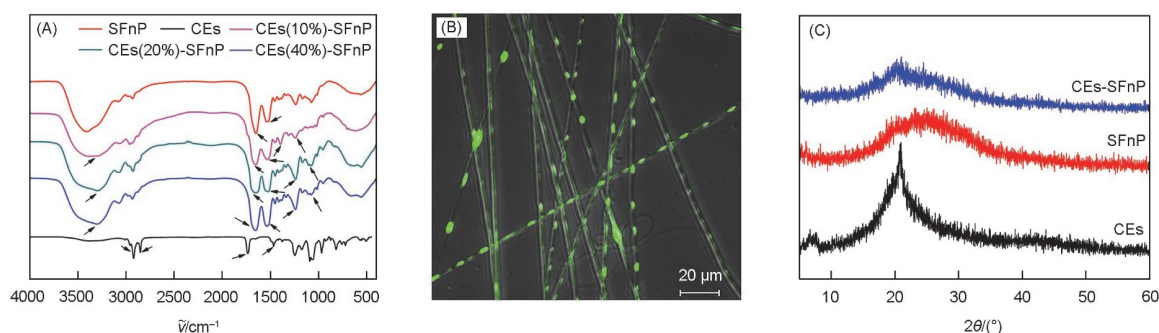


**Fig.3** FTIR spectra(A), fluorescent image(B) and XRD patterns(C) of the electrospun CE-SF nPs

It can be seen from Fig.3(C) that CEs have an amorphous diffraction peak at about  $2\theta=20^\circ$  and the SF nanofiber has an amorphous diffraction peak at  $2\theta=24^\circ$ , while the diffraction peak of CE-SF nPs moved to the left, indicating that the interaction between SF molecules and CEs leads to the change of the diffraction peak. Since ethanol has been reported causing the transformation of SF structure from random coil to  $\beta$ -sheet<sup>[15]</sup>, the ethanol contained in the CEs may have played a role in promoting the left shift of the peak.

The relationship between CE-SF nPs and temperature change under program temperature control was also investigated. The result is shown in Fig.4. The mass loss of the CE-SF nPs composite nanofibers can be divided into three stages. The first stage was between 40 and 100 °C and mainly the dehydration stage of the composite nanofiber membrane, during which the mass loss was caused by the residual moisture in the composite nanofibers and the evaporation of ethanol in the CEs<sup>[20]</sup>. The second stage is at 147 °C when egg yolk lecithin in the CEs started to decompose. The third stage is 278—600 °C, where the mass loss of the composite

nanofibers was the fastest, which was mainly caused by the destruction of the side chain and the main chain of SF molecules<sup>[21]</sup>. It can also be seen from the thermogravimetric curves that the thermal decomposition process of the CE-SF nPs was completed in one step, indicating that the composite of CEs and SF is thermo-dynamically compatible. The thermodynamic properties of different materials were then calculated based on the TG curves. As shown in Table S2 (see the Electronic Supplementary Material of this paper), the addition of a small amount of CEs did not have much effect on the initial decomposition temperature of SF nanofibers.

### 3.3 Cytocompatibility of CE-SF nP

Mouse skin fibroblasts L929 were used to assess the cytocompatibility of CE-SF nP. As shown in Fig.5(F), the proliferation of the skin cells grown on the CE-SF nPs is significantly faster than that on the glass. Also, the cells on the CE-SF nPs presented a typical fully spread morphology, bridging each

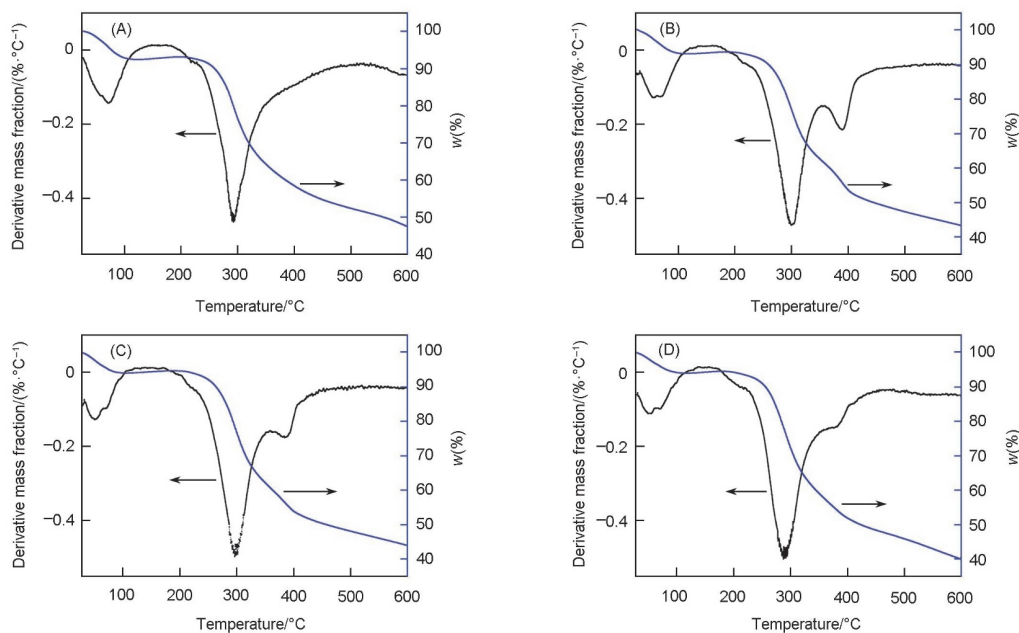


**Fig.4 Thermogravimetric curves of the CEs-SFNPs**  
(A) SF; (B) CEs(10%)-SFnP; (C) CEs(20%)-SFnP; (D) CEs(40%)-SFnP.

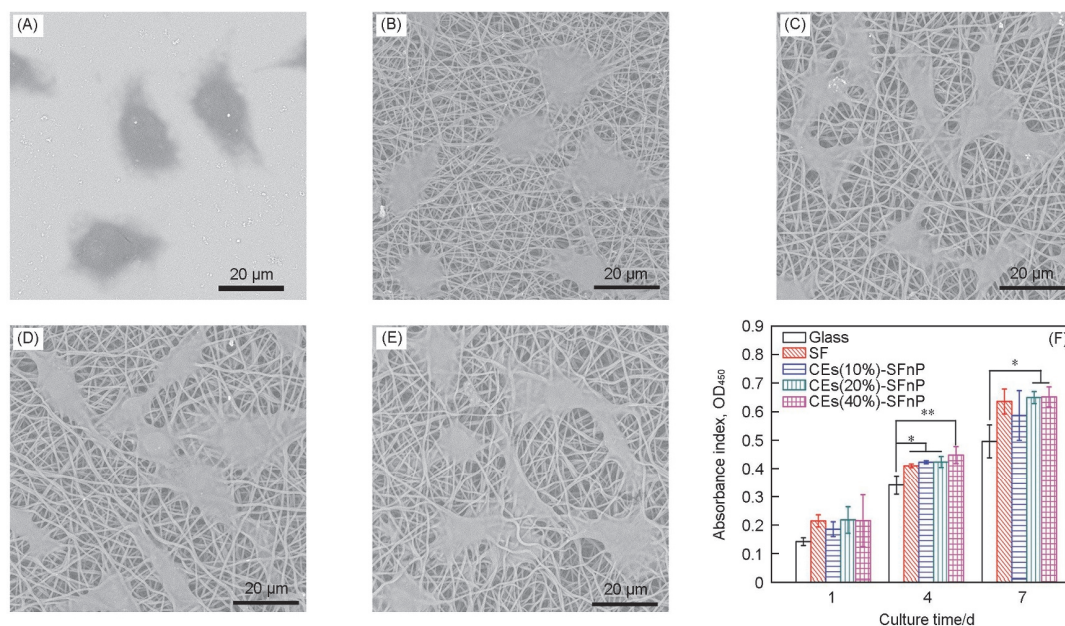


**Fig.5 SEM images(A—E) and viabilities(F) of L929 cells grown on different substrates**  
(A) Glass; (B) SF; (C) CEs(10%)-SFnP; (D) CEs(20%)-SFnP; (E) CEs(40%)-SFnP. \*  $P < 0.05$ ; \*\*  $P < 0.01$ .

other to form a cell sheet; while the cells growing on the glass did not spread significantly and showed a relatively isolated growth pattern[Fig.5(A—E) and Fig.S3, see the Electronic Supplementary Material of this paper]. The cells fully spread to bridge each other could be beneficial to the signal transduction between cells and nanofibers, which greatly enhanced proliferation of cell<sup>[11,22]</sup>. These results indicate that the as-spun CEs-SFNPs have a good cytocompatibility, and the addition of an appropriate amount of CEs does not impair the cytocompatibility of SF.

### 3.4 Transdermal Drug Delivery Performance

With Dox used as a model drug, the transdermal drug delivery performance of the drugs@CEs loaded SFnP was investigated. Fig.6 shows the cumulative release of Dox against the mouse skin from the Dox@CEs-SFnP and Dox@SFnP. At each time point, the amount of drug released from Dox@CEs-SFnP was much higher than that in Dox@SFnP, indicating that the transdermal drug delivery efficiency of the former is

significantly better than that of the latter. After the transdermal drug release experiment, the skin samples were made into slices and examined on an LSCM. As shown in Fig.7, the fluorescence intensity of the skin samples(both the cross-section and longitudinal section) from Dox@CEs-SFnP group is significantly higher than that of Dox@SFnP group, indicating that more drugs are retained in the skin tissue after being administered percutaneously with Dox@CEs-SFnP. These results demonstrate that CE-SFnP has good performance in

transdermal drug delivery.

Because it contains low-molecular-weight alcohol, Eth can be flexibly deformed to facilitate penetration of the stratum corneum into the deep layer of the skin<sup>[23,24]</sup>. The introduction of octadecylamine makes CEs positively charged, which facilitates its adsorption on the negatively charged cell membrane and promotes the integration between them. Our data confirmed the good transdermal performance of CEs. Since the CEs solution or its dry powder is inconvenient to use,

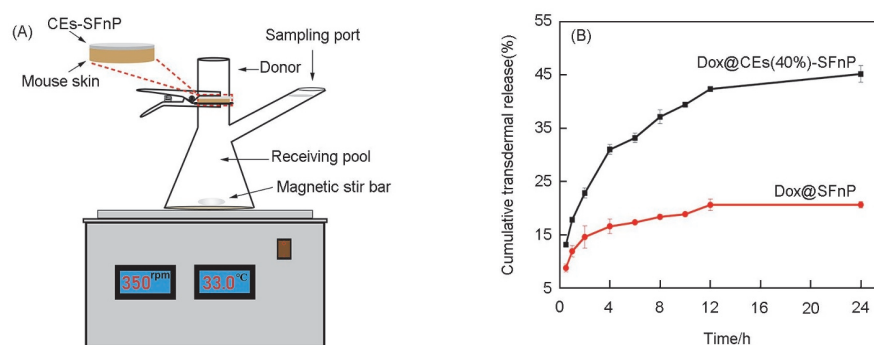


**Fig.6** Schematic diagram of the transdermal experiment with Franz diffusion cell(A) and cumulative release of Dox through the mouse skin(B)

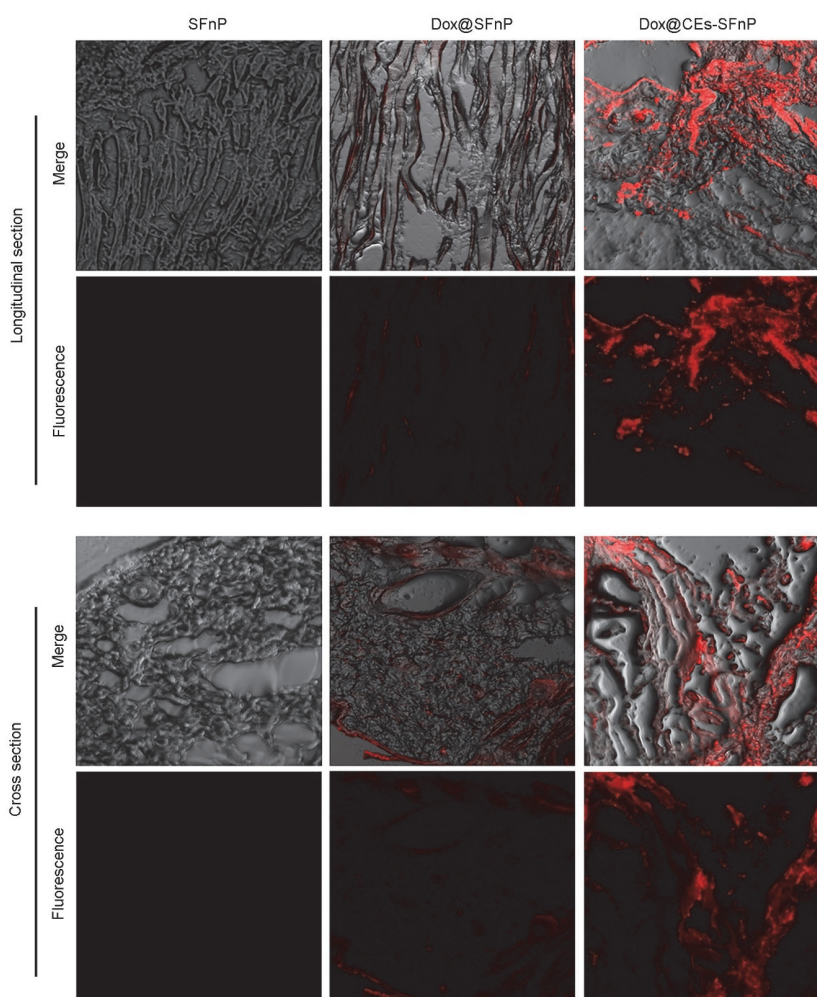


**Fig.7** Micrographs of the skin tissue section showing the intradermal retention of Dox

it is necessary to configure a suitable support substrate for the CEs. The SF nanofibers have large specific surface area and excellent skin affinity<sup>[9,13–15]</sup>, which make the SFnP a good substrate for CEs. Here, we demonstrate that the TDDS based on CEs-SFnP is effective on delivering drugs percutaneously.

## 4 Conclusions

A novel TDDS based on the green electrospun CEs-SFnP was reported in this study. The CEs have a good stability and a high encapsulation efficiency. With drugs encapsulated in the CEs, the CEs-SFnP showed a good performance in delivery of drugs percutaneously. In view of its good transdermal performance, excellent skin affinity and easy and eco-friendly fabrication, the as-spun CEs-SFnP could find a promising application potential in TDDS.

## Electronic Supplementary Material

Supplementary material is available in the online version of this article at <http://dx.doi.org/10.1007/s40242-021-1084-8>.

## Acknowledgements

This work was supported by the Project of the Science & Technology Commission of Shanghai Municipality, China (Nos.18490740400, 20DZ2254900).

## Conflicts of Interest

The authors declare no conflicts of interest.

## References

- [1] Cevc G., Vierl U., *Journal of Controlled Release*, **2010**, *141*, 277
- [2] Mitragotri S., *Adv. Drug Deliv. Rev.*, **2004**, *56*, 555
- [3] Touitou E., Bergelson L. G. B., Eliaz M., Dayan N., *Journal of Controlled Release*, **2000**, *65*, 403
- [4] Zhou X., Hao Y., Yuan L., Pradhan S., Shrestha K., Pradhan O., Liu H., Li W., *Chinese Chemical Letters*, **2018**, *29*, 1713
- [5] Kulkarni M., Greiser U., O'Brien T., Pandit A., *Trends in Biotechnology*, **2010**, *28*, 28
- [6] Stevens M., George J., *Science*, **2005**, *310*, 1135
- [7] Huang H., He C., Wang H., Mo X., *Journal of Biomedical Materials Research Part A*, **2009**, *90*, 1243
- [8] Yan S., Li X., Tan L., Mo X., *Polymer*, **2009**, *50*, 4212
- [9] Fan L., Wang H., Zhang K., Cai Z., He C., Sheng X., Mo X., *RSC Advances*, **2012**, *2*, 4110
- [10] Yan S., Li X., Liu S., Mo X., Ramakrishna S., *Colloids and Surfaces B: Biointerfaces*, **2009**, *73*, 376
- [11] Sobajo C., Behzad F., Yuan X., Bayat A., *Eplasty*, **2008**, *8*, 438
- [12] Vepari C., Kaplan D. L., *Prog. Polym. Sci.*, **2007**, *32*, 991
- [13] Yang X., Fan L., Ma L., Wang Y., Lin S., Yu F., Pan X., Luo G., Zhang D., Wang H., *Materials & Design*, **2017**, *119*, 76
- [14] Fan L., Cai Z., Zhang K., Han F., Li J., He C., Mo X., Wang X., Wang H., *Colloids and Surfaces B: Biointerfaces*, **2014**, *117*, 14
- [15] Sheng X., Fan L., He C., Zhang K., Mo X., Wang H., *International Journal of Biological Macromolecules*, **2013**, *56*, 49
- [16] Rakesh R., Anoop K. R., *J. Pharm. Bioallied Sci.*, **2012**, *4*, 333
- [17] Ma L., Wang X., Wu J., Zhang D., Zhang L., Song X., Hong H., He C., Mo X., Wu S., Kai G., Wang H., *Nanomedicine(Lond)*, **2019**, *14*, 2395
- [18] Steffi C., Wang D., Kong C. H., Wang Z., Lim P. N., Shi Z., Thian E. S., Wang W., *ACS Applied Materials & Interfaces*, **2018**, *10*, 9988
- [19] Yu D., Yang J., Wang X., *Nanotechnology*, **2012**, *23*, 105606
- [20] Shchipunov Y. A., Shumilina E. V., *Materials Science & Engineering C*, **1995**, *3*, 43
- [21] Müller V., Certari M., Palácio S. M., Campos S. D. D., Muniz E. C., Campos E. A. D., *Journal of Applied Polymer Science*, **2015**, *132*, 41717
- [22] Roh D. H., *Journal of Materials Science: Materials in Medicine*, **2006**, *17*, 547
- [23] Dayan N., Touitou E., *Biomaterials*, **2000**, *21*, 1879
- [24] Godin B., Touitou E., *Journal of Controlled Release*, **2004**, *94*, 365